NASA TECHNICAL MEMORANDUM

NASA TM X-3109

NASA TM X-3109

CALCULATION OF THE PRESSURE DISTRIBUTION ON AXISYMMETRIC BOATTAILS INCLUDING EFFECTS OF VISCOUS INTERACTIONS AND EXHAUST JETS IN SUBSONIC FLOW

by Josef Rom and Lawrence J. Bober

Lewis Research Center
Cleveland, Ohio 44135

NATIONAL AERONAUTICS AND SPACE ADMINISTRATION • WASHINGTON, D. C. • SEPTEMBER 1974

1. Report No.	2. Government Accession No.	3. Recipient's Catalog No.
NASA TM X-3109		

4. Title and Subtitle	5. Report Date
CALCULATION OF THE PRESSURE DISTRIBUTION ON AXISYMMETRIC BOATTAILS INCLUDING EFFECTS OF VISCOUS INTERACTIONS AND EXHAUST JETS IN SUBSONIC FLOW	SEPTEMBER 1974
	6. Performing Organization Code

7. Author(s)	8. Performing Organization Report No.
Josef Rom, Technion-Israel Institute of Technology, Haifa, Israel; and Lawrence J. Bober; Lewis Research Center	E-7811
	10. Work Unit No. 501-24

9. Performing Organization Name and Address	11. Contract or Grant No.
Lewis Research Center National Aeronautics and Space Administration Cleveland, Ohio 44135	
	13. Type of Report and Period Covered: Technical Memorandum

12. Sponsoring Agency Name and Address	14. Sponsoring Agency Code
National Aeronautics and Space Administration Washington, D.C. 20546	

15. Supplementary Notes

16. Abstract

A method of calculating the pressure distributions on boattails is proposed. This method accounts for viscous effects including the presence of a separated region for base flows by combining an inviscid analysis with a boundary layer analysis in an iterative calculation. Details of the reversed flow region are not considered. Some preliminary results have been obtained for boattails at subsonic free stream Mach number with turbulent boundary layers separating at the boattail base. In some cases convergence could not be obtained using the present computer program. It is possible, in principle, to extend this method to the calculation of boattail flows with pressure gradient induced separation on the boattail.

17. Key Words (Suggested by Author(s))	18. Distribution Statement
Subsonic flow; Turbulent boundary layer; Base flow; Separated flow; Viscous-inviscid interaction	Unclassified - unlimited Category 01

19. Security Classif. (of this report)	20. Security Classif. (of this page)	21. No. of Pages	22. Price*
Unclassified	Unclassified	20	$3.00

* For sale by the National Technical Information Service, Springfield, Virginia 22151

CALCULATION OF THE PRESSURE DISTRIBUTION ON AXISYMMETRIC BOATTAILS INCLUDING EFFECTS OF VISCOUS INTERACTIONS AND EXHAUST JETS IN SUBSONIC FLOW

by Josef Rom* and Lawrence J. Bober

Lewis Research Center

SUMMARY

An approximate method of calculating the pressure distributions on boattails has been proposed. This method accounts for viscous effects including the presence of a separated region for base flows by combining an inviscid analysis with a boundary layer analysis in an iterative calculation. Details of the reversed flow region are not considered; instead, the reversed flow region is considered as a solid body and the streamwise flow is treated as a boundary layer. The shape of the dividing line between the streamwise and reverse flow regions is calculated by an iteration procedure. This method requires that the static pressure at the separation point (boattail trailing edge pressure) be specified. It is possible, in principle, to extend this method to the calculation of boattail flows with pressure gradient induced separation on the boattail.

Some preliminary results have been obtained for boattails at subsonic free stream Mach numbers with turbulent boundary layers separating at the boattail base. A computer program based on an iterative calculation between an integral turbulent boundary layer method and a subsonic potential flow method was used. In some cases, reasonable agreement was obtained for both the boattail pressure distribution and the pressure drag when the calculated pressure just ahead of the base was matched to the measured pressure at the same location. In other cases, convergence was not obtained.

---

* Professor of Aeronautical Engineering, Technion-Israel Institute of Technology, Haifa, Israel.

INTRODUCTION

The drag and the pressure distributions on the boattailed afterbodies of flight vehicles and of engines are of considerable importance for evaluation of the optimal flight configurations. The engine afterbody drag rise must also be evaluated at conditions with jet exhaust. Some methods for evaluation of the boattail drag and some experimental data on various boattails at subsonic, transonic, and supersonic speeds are presented in references 1 to 4. The methods for evaluation of the boattail pressure distribution are based on inviscid flow field calculations, sometimes with corrections due to viscous effects.

The present analysis considers the flow over the boattail of an axisymmetric body. The flow is assumed to consist of a viscous layer near the body and extending into the wake and the external flow which is essentially inviscid. The effect of the viscous layer near the body is taken into account by modifying the body shape by an appropriate displacement thickness and the effect of the wake by determining an equivalent body in the wake region.

In the framework of this representation the jet effects as well as boundary layer separation on the boattail surface is accounted for by a properly shaped afterbody simulating the wake. The afterbody shape is selected to yield the known pressure at the boattail base. More elaborate interaction calculations can be devised so that no specific pressure reference would be required. However, the present calculation scheme requires that a base pressure be specified.

SYMBOLS

C_p	pressure coefficient
C_{p_b}	base pressure coefficient (taken as pressure coefficient at last boattail point at which pressure was calculated)
D	maximum model diameter
M_0	free stream Mach number
P_{tj}/p_o	ratio of jet total pressure to free stream static pressure
R	radius of body on which pressure is calculated, $r + \delta^*/\cos \alpha$
r	radius of body on which boundary layer is calculated
s	separation point location
u	tangential component of velocity

u_b	maximum backflow velocity
x	axial distance from start of boattail
α	local surface angle
β	boattail trailing edge angle
δ^*	displacement thickness
$\Delta\alpha_b$	initial flow turning angle at base

Subscripts:

b	on body
ds	dividing streamline
e	at edge of boundary layer
fs	free shear layer
i	iteration number
o	minimum value
smooth	region where displacement surface was smoothed
w	in wake

METHOD OF ANALYSIS

Separation at Base

The basic hypothesis in the present flow model is presented in figure 1.

The flow is divided into the following regions:

(1) Inviscid flow around the corrected body.

(2) Viscous flow:

(a) Upstream of base, the boundary layer calculation is made on the solid boundaries of the model (for cases with no separation boattail).

(b) Downstream of base, a zero velocity line is assumed, defining a fictitious afterbody. On this new shape the boundary layer calculation is continued until the results diverge as $r_w(x) \to 0$. At the minimum value of $R_w(x)$ a cylindrical afterbody is assumed having a radius R_{w_o}. Henceforth, this afterbody will be referred to as the "wake-body."

The new body shape is now defined by a continuous curve starting with $R_b = r_b + \delta_b^*/\cos\alpha_b$ on the body and $R_w = r_w + \delta_w^*/\cos\alpha_w$ in the near wake termi-

nating in a cylindrical body of radius r_{w_o} as $x \to \infty$ (fig. 1). The shape of the line $u = 0$, that is, the coordinates $r_w(x)$, is modified in the iteration procedure until the viscous-inviscid interaction calculation is convergent. This iteration procedure is described in a later section. The final wake shape is determined such that the converged value of the base (boattail trailing edge) pressure is equal to the prescribed base (trailing edge) pressure.

Separation on Boattail

Although calculation of this type of flow has not been attempted with the present analysis, it is in principle similar to the calculation of flow separating at the base. However in this case, the initial boundary layer calculation will indicate separation at the point "s" shown in figure 2 and it will be necessary to start the "wake-body" at this location. In the iteration procedure for this type of flow, not only the shape of the zero velocity line, but also the location of the separation point would change from iteration to iteration. When convergence is obtained, the boundary layer calculation should indicate conditions of incipient separation at the separation point but then continue along the zero velocity line as an attached boundary layer.

Justification of the "Wake-Body" Model

The use of the "wake-body" model in the iteration calculation requires the following approximations:

(1) Define the $u = 0$ line in the wake as a streamline defining an equivalent body. This means neglecting the normal velocity on the $u = 0$ line.

(2) Assume that the velocity profile above the $u = 0$ line is the turbulent boundary layer profile.

(3) Neglect the reverse flow region below the $u = 0$ line.

Using the $u = 0$ line instead of the dividing streamline to define an inviscid body shape may be justified in cases of shallow separated zones as shown in figure 3. The definition of the dividing streamline requires that the mass flow between the $u = 0$ line and the dividing streamline equal the mass flow between the $u = 0$ line and the axis of the body. If the density variation in the wake is small, the definition of the dividing streamline implies that

$$\frac{\delta_r}{r_w} \sim 0\left(\frac{u_b}{u_{ds}}\right) \tag{1}$$

where δ_r is the distance between the $u = 0$ line and the dividing streamline, u_b is the maximum backflow velocity, and u_{ds} is the velocity on the dividing streamline. The backward flow velocity u_b in the "dead water" zone is extremely difficult to evaluate accurately. Some calculations of this reverse flow velocity in two-dimensional laminar separated flows are presented in references 5 and 6. There extremely low values of u_b/u_e were obtained, that is $u_b/u_e \sim 0.02$ to 0.04. An experimental measurement of the reverse flow profile in a separated flow on a two-dimensional airfoil in turbulent subsonic and transonic flows is presented in reference 7, where values of u_b/u_e of about 0.15 are obtained. The velocity on the dividing streamline is determined in reference 8 to be about 0.528 u_e for incompressible two-dimensional laminar flow. The value of u_{ds} in incompressible turbulent flow is about 0.61 u_e (ref. 9). These result in u_b/u_{ds} values of about 0.03 to 0.28. From equation (1), it can be seen that δ_r is small compared to r_w and the assumption that the $u = 0$ line is a streamline is reasonable.

Since the velocity profiles of turbulent shear flow and the turbulent boundary layers are not significantly different, the difference between the displacement thicknesses in both cases is even smaller so that the assumption $\delta^* \cong \delta^*_{fs}$ is reasonable and the present approximation in determining a corrected shape for the inviscid calculation may be expected to produce reasonable results.

As noted previously, the definition of an equivalent solid body on the $u = 0$ line introduces an approximation to the boundary conditions in evaluating the viscous flow distribution in the boundary layer in comparison to those experienced in the actual free shear layer. In the actual free shear layer there is flow normal to the $u = 0$ line since this is not actually a streamline. In the present model the normal component of velocity is assumed to be zero. This effect is assumed to have a small effect on the displacement thickness.

A result of these approximations is that, since the mixing process in the wake is not correctly taken into account, a unique location of the $u = 0$ line is not obtained. It can be shown that convergent solutions can be obtained for various shapes of the $u = 0$ line each resulting in a different base pressure. It seems likely that for each calculated value of base pressure, the calculated pressure distribution on the boattail upstream of the base and probably also in the wake near the base is correct. This feature allows the calculation of pressure distributions on the boattail including the effect of a jet plume. Here it is assumed that there is a relation between the jet pressure and the boattail base pressure. An a posteriori justification for this assumption can be found in comparison of the calculated pressure distributions with experimental data with and without jet plumes discussed later in this report.

Some corrections to the present model can be obtained by modifying the boundary layer computation downstream of the base. This modification may be done by using velocity profiles calculated for shear layers or even a calculated reverse profile. In

addition the boundary conditions on the $u = 0$ line can be made more correct by including an estimated normal velocity component at this boundary (similar to the injection condition). However, since any of these corrections required considerable modifications in the presently available computer programs, it was deemed more important at this stage to proceed with the available computer programs using the simplifying assumptions in order to develop the calculation procedure for the interaction model. Some of the corrections may be incorporated in future studies.

Calculation Procedure

Viscous flow program. - The flow model used in the interaction calculations requires an evaluation of a boundary layer displacement thickness. This displacement thickness is related to the external flow pressure distribution and to the boundary conditions on the body surfaces (heat transfer, mass injection, or suction, etc.) through the boundary layer equations. In subsonic and transonic flows on boattails under most flight conditions the boundary layer is fully turbulent well ahead of the boattail. Therefore only the turbulent boundary layer case will be considered. There are a number of reasonable methods for evaluation of turbulent boundary layers. Some of these are reported in references 10 to 13.

Due to its simplicity and ready availability, a computer program using the method of Sasman and Cresci (ref. 10) was utilized in the present investigation. Since this is an integral method, this program is relatively short but still results in good boundary layer calculations as indicated in the AFOSR-IFP Stanford Conference (ref. 14) and can carry through reasonable adverse pressure gradients.

Future programs based on finite difference schemes may be amenable to a more refined interaction calculation. However, for the evaluation of the proposed interaction scheme the present boundary layer program is adequate.

Inviscid flow program. - The flow over the corrected body is calculated by a program for the solution of the subsonic potential flow equations based on the Neumann method (ref. 15). This method enables an exact calculation of the pressure distribution on axially symmetric bodies. It is important to note that in order to obtain good results in viscous-inviscid interaction calculations one should use exact full equations rather than linearized equations for the external flow. This may be similar to the requirement of using a full characteristic solution in the supersonic interaction case as discussed by Miller (ref. 16). The program of reference 15 for flows over bodies at subsonic speeds has been shown to give very accurate results. In this case again the program was readily available.

Viscous-inviscid calculation procedure. - Calculation procedures have been devel-

oped for the interactive flow based on the flow model for the case of separation at the base (fig. 1). The problem of separation on the boattail (fig. 2) has not yet been attacked.

The calculation is started using the inviscid flow program with uncorrected body coordinates. In order to perform this calculation in subsonic flow, conditions downstream of the body's base have to be included. As discussed previously, the introduction of the "wake-body" approximation defines the body's coordinates in that region. The calculated pressure distribution is used as input to the boundary layer method to determine the displacement thickness. The displacement thickness is added to the body coordinates and zero velocity line in the wake. There are two problematic zones that require special computing procedures.

(1) In the reattachment zone where the line $u = 0$ reaches the axis, the boundary layer thickness and displacement thickness increase to infinity. A cylindrical body is defined with radius R_{w_o} which is equal to the minimum radius of the displacement surface (indicated in figs. 1 and 2).

(2) At the boattail base, due to a sharp expansion, the displacement surface exhibits strong variations of the local slope causing oscillations of the pressure. These oscillations increase in each additional iteration as seen in figure 4(a). This appears to be an artificial oscillation caused by the sensitivity of the inviscid flow program to discontinuity in boundary slopes. It was found that by smoothing out this region by proper curve fitting these oscillations can be eliminated and the computation scheme made to converge. The effect of smoothing using 2, 4, 6, and 8 points is shown in figure 4(b), (c), (d), and (e), respectively. The region in which the smoothing was performed is indicated in the figure. For the conditions shown in figure 5, using eight-point smoothing results in an extremely small variation of the local pressure and therefore good convergence of the computational process. The effect of smoothing various numbers of points on the convergence of the boattail pressure drag is shown in figure 5.

Since the shape of the "wake-body" is not known, the $u = 0$ line is corrected in each iteration as follows:

(1) Start with an arbitrary shape for the $u = 0$ line.

(2) Compute the pressure distribution and $\delta^*(x)$ for this body shape.

(3) Determine a corrected body by the following scheme.

(a) For the first iteration ($i = 1$)

(i) On the body: $R_{b_{i+1}}(x) = r_b(x) + \delta^*_{b_i}(x)/\cos \alpha_b(x)$

(ii) In the wake: $R_{w_{i+1}}(x) = r_{w_i}(x) + \delta^*_{w_i}(x)/\cos \alpha_{w_i}(x)$

(b) For successive iterations ($i > 1$)

(i) On the body: $R_{b_{i+1}}(x) = r_b(x) + \delta^*_{b_i}(x)/\cos \alpha_b(x)$

(ii) In the wake: $r_{w_{i+1}}(x) = R_{w_i}(x) - \delta^*_{w_i}(x)/\cos \alpha_{w_i}(x)$ and

$$R_{w_{i+1}}(x) = r_{w_{i+1}}(x) + \delta^*_{w_{i+1/2}}(x)/\cos \alpha_{w_{i+1/2}}(x).$$

Here r is the radius of the surface on which the boundary layer is calculated, R is the radius of the displacement surface, the subscripts b and w refer to the body and wake, respectively, and the subscript i denotes the iteration number. This scheme is shown schematically in figure 6.

The convergence of the solution for a typical initial shape of the $u = 0$ line is found to be reasonably fast as seen in figure 7. For all results shown in this report, the initial shape of the $u = 0$ line was specified in the following manner. The slope of the first straight line segment in the wake was taken to be the same as the slope of the last segment on the boattail. (The inviscid analysis (ref. 11) represents the body by a series of straight line segments.) Each of the next three segments was at an angle of $\Delta\alpha_b/3$ with respect to the segment upstream of it. The remainder of the $u = 0$ line was taken to be a straight line. The lengths of the segments were smallest near the base and increased gradually in the downstream direction. Distributing the turn over a number of points was done to avoid excessively strong pressure gradients in the first iteration which might cause the initial boundary layer calculation to indicate separation.

The present procedure will result in a convergent solution for any reasonable initial $u = 0$ line since no criterion for wake structure is included in the present flow model. The various pressure distributions which are obtained at convergence on various initial $u = 0$ lines are shown in figure 8. These pressure distributions are characteristic of those obtained with different jet pressure ratios. If a correspondence between base pressure coefficient and jet pressure ratio can be determined, then the pressure distributions shown in figure 9 can be attributed to specific jet pressure ratios. The dependence of the base pressure on the jet pressure ratio (including the jet off condition) can be obtained from other analyses or from experimental data (such as those in ref. 1). A value of jet pressure ratio can be attributed to each of the curves in figure 8 by comparing the pressure at the end of the boattail (which is approximately equal to the base pressure) on these curves to the base pressures at known jet pressure ratios. Having this information then allows the calculation of the complete boattail pressure distribution at any value of jet pressure ratio.

An interesting variation of the pressure distribution and particularly the base pressure as a function of the initial "wake-body" deflection angle, $\Delta\alpha_b$, is found in this analysis. The variation of the base pressure C_{p_b} as a function of $\Delta\alpha_b$ is shown in figure 9 for a 10° conical boattail. It is found that C_{p_b} has a minimum value for a certain "wake-body" angle. Although the same base pressure is obtained for two

different $\Delta\alpha_b$ (away from the minimum), the pressure distributions are different.

The behavior of these solutions is apparently due to the influence of the recompression in the wake on the boattail pressures. For positive values of the initial turning angle at the base $\Delta\alpha_b$, the recompression of the flow in the wake as $R \to R_o$ is far removed from the base. As a result the flow near the end of the boattail is determined primarily by the conditions in the vicinity of the base. Thus, as $\Delta\alpha_b$ becomes smaller, less recompression occurs at the base causing a decrease in pressure. This in turn causes a thinning of the boundary layer and a further drop in pressure near the end of the boattail. When $\Delta\alpha_b$ has decreased by a large enough amount, the recompression in the wake is close enough to the base to have as strong an effect on the boattail pressures as the expansion at the base. Then as $\Delta\alpha_b$ is decreased further, the pressure near the end of the boattail rises as the recompression in the wake becomes stronger and closer to the boattail. This causes the boundary layer near the end of the boattail to grow more rapidly, resulting in a further increase in pressure. The significance of this pressure coefficient minimum is not clear since it does not correspond to a particular flow condition such as the jet off case.

RESULTS AND DISCUSSION

The present method has been applied to the calculation of the pressure distribution and pressure drag of conical afterbodies at subsonic speeds for a limited number of cases. These cases did not have separated flow on the conical afterbodies. The calculated pressure at the last input point on the boattail was matched to the pressure obtained at the same location from a curve drawn through the measured pressures on the boattail. The data shown in the following comparisons are from reference 1.

Shown in figure 10 are the theoretical and experimental static pressure distributions for a 3° conical boattail at a free stream Mach number of 0.8. The ratio of nozzle exit to throat area for this configuration was 1.721. The three upper curves and data correspond to different values of exhaust jet total to free stream static pressure ratio; the lowest curve and data correspond to the jet off condition. Good agreement was obtained for the jet off condition; for the jet on conditions the agreement was not as good. The best agreement for the three jet on cases was obtained at the highest pressure ratio.

Theoretical and experimental pressure drag coefficients corresponding to the pressure distributions of figure 10 are shown in figure 11. The drag coefficients are plotted against the base pressure coefficient since the analysis uses base pressure as an independent variable. The analysis yields drag coefficients that are in reasonable agreement with those obtained experimentally.

Results for a 10° conical boattail at a free stream Mach number of 0.4 are shown

in figure 12. The ratio of nozzle exit to throat area was 1.112. Theoretical and experimental static pressure distributions are shown for only two jet pressure ratios. The experimental base pressure coefficient for the jet off condition was lower than the minimum calculated value shown in figure 10 and therefore no comparison is made for this condition.

Pressure drag coefficients are shown in figure 13 for the 10° conical boattail at free stream Mach numbers of 0.4 and 0.8. The $M_0 = 0.4$ results correspond to the pressure distributions shown in figure 12. The $M_0 = 0.8$ results are shown for the fourth iteration even though the calculations could not be forced to converge at this condition. This is done so that attention can be drawn to two problem areas in the analysis. First, it can be seen that the number of points used in the smoothing at the base affects the drag level especially at the higher base pressures which correspond to higher jet pressure ratios. Second, the drag level is considerably lower than the experimental values. This is caused by the inability of the method to properly predict the pressure in the strong overexpansion at the start of the boattail region. For the 10° boattail at $M_0 = 0.4$ and the 3° boattail at $M_0 = 0.8$, the expansions are not as strong and good agreement is obtained at the shoulder (figs. 10 and 11). The overexpansion which occurs at the sharp corner at the start of the boattail may require the use of viscous layer equations which include the effects of normal pressure gradients.

Calculations were also made for a 15° conical boattail at $M_0 = 0.4$ but results are not shown since satisfactory convergence could not be obtained even by smoothing 12 points at the base. Smoothing more points was deemed inappropriate.

SUMMARY OF RESULTS

An approximate method of calculating the pressure distributions on boattails has been proposed. This method accounts for viscous effects including the presence of a separated region for base flows by combining an inviscid analysis with a boundary layer analysis in an iterative calculation. Details of the reversed flow region are not considered; instead, the reversed flow region is considered as a solid body and the streamwise flow is treated as a boundary layer. The shape of the dividing line between the forward and reverse flow regions is calculated by an iteration procedure. This method requires that the static pressure at the separation point be specified. It is possible, in principle, to extend this method to the calculation of boattail flows with pressure gradient induced separation on the boattail.

Some preliminary results have been obtained for boattails at subsonic free stream Mach numbers with turbulent boundary layers separating at the boattail base. A computer program based on an iterative calculation between an integral turbulent boundary layer method and a subsonic potential flow method was used. Results are compared to

the measured pressure distribution on a 3° conical boattail at a free stream Mach number of 0.8 and a 10° conical boattail at a free stream Mach number of 0.4 for various jet pressure ratios. Reasonable agreement was obtained for both the boattail pressure distribution and the boattail pressure drag when the calculated pressure just ahead of the base was matched to the measured pressure at the same location. Oscillations of the pressure near the base were eliminated by smoothing the displacement surface a short distance upstream and downstream of the base. For higher angle boattails, this smoothing did not result in convergence of the pressure distribution.

Lewis Research Center,
National Aeronautics and Space Administration,
Cleveland, Ohio, June 18, 1974,
501-24.

REFERENCES

1. Compton, William B., III; and Runckel, Jack F.: Jet Effects on the Boattail Axial Force of Conical Afterbodies at Subsonic and Transonic Speeds. NASA TM X-1960, 1970.

2. Fox, Charles H., Jr.: Experimental Surface Pressure Distributions for a Family of Asymmetric Bodies at Subsonic Speeds. NASA TM X-2439, 1971.

3. Compton, William B., III: Jet Effects on the Drag of Conical Afterbodies at Supersonic Speeds. NASA TN D-6789, 1972.

4. Reubush, David E., and Runckel, Jack F.: Effect of Fineness Ratio on the Boattail Drag of Circular-Arc Afterbodies Having Closure Ratios of 0.5 with Jet Exhaust at Mach Numbers up to 1.30. NASA TN D-7192, 1973.

5. Catherall, D.; and Mangler, K. W.: The Integration of the Two-Dimensional Laminar Boundary-Layer Equations Past the Point of Vanishing Skin Friction. J. Fluid Mech., vol. 26, pt. 1, Sept. 1966, pp. 163-182.

6. Briley, W. R.: A Numerical Study of Laminar Separation Bubbles Using the Navier-Stokes Equations. J. Fluid Mech., vol. 47, pt. 4, June 20, 1971, pp. 713-736.

7. Alber, I. E.; Bacon, J. W.; Masson, B. S.; and Collins, D. J.: An Experimental Investigation of Turbulent Transonic Viscous-Inviscid Interactions. AIAA J., vol. 11, no. 5, May, 1973, pp. 620-627.

8. Chapman, D. R., Kuehn, D. M., and Larsen, H. K.: Investigation of Separated Flows in Supersonic and Subsonic Streams with Emphasis on the Effects of Transition. NACA TR 1356, 1958.

9. Rom, J.; and Levi, E.: The Semi-Empirical Parameters Used in the Dividing Streamline and the Momentum Integral Analyses for Separated Flows. Israel J. Technol., vol. 7, no. 1-2, 1969, pp. 163-171.

10. Sasman, Philip K.; and Cresci, Robert J.: Compressible Turbulent Boundary Layer with Pressure Gradient and Heat Transfer. AIAA J., vol. 4, no. 1, Jan. 1966, pp. 19-25.

11. Bradshaw, P.; Ferris, D. H.; and Atwell, N. P.: Calculation of Boundary-Layer Development Using the Turbulent Energy Equation. J. Fluid Mech., vol. 28, part 3, May 26, 1967, pp. 593-616.

12. Herring, H. J.; and Mellor, G. L.: Computer Program for Calculating Laminar and Turbulent Boundary Layer Development in Compressible Flow. NASA NASA CR-2068, 1972.

13. Cebeci, T.; and Smith, A. M. O.: A Finite-Difference Method for Calculating Compressible Laminar and Turbulent Boundary Layers. J. Basic Eng., vol. 92, no. 3, Sept., 1970, pp. 523-535.

14. Kline, S. J., Morkovin, M. V., Sovran, G., and Cockrell, D. J., eds.: Computation of Turbulent Boundary Layers; Proceedings of the AFOSR-IFP-Stanford Conference, Stanford University, Stanford, Calif., August 18-25, 1968. Stanford Univ. Press, 1968.

15. Hess, J. L.; and Smith, A. M. O.: Calculation of Potential Flow About Arbitrary Bodies. Progress in Aeronautical Sciences, Vol. 8. D. Kuchemann, ed., Pergamon Press. 1967, pp. 1-138.

16. Miller, G.: Mathematical Formulation of Viscous-Inviscid Interaction Problems in Supersonic Flow. AIAA J., vol. 11, no. 7, July 1973, pp. 938-942.

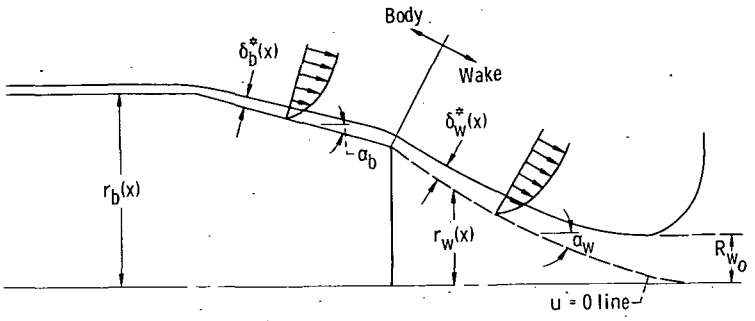

Figure 1. - "Wake-body" model (separation at base).

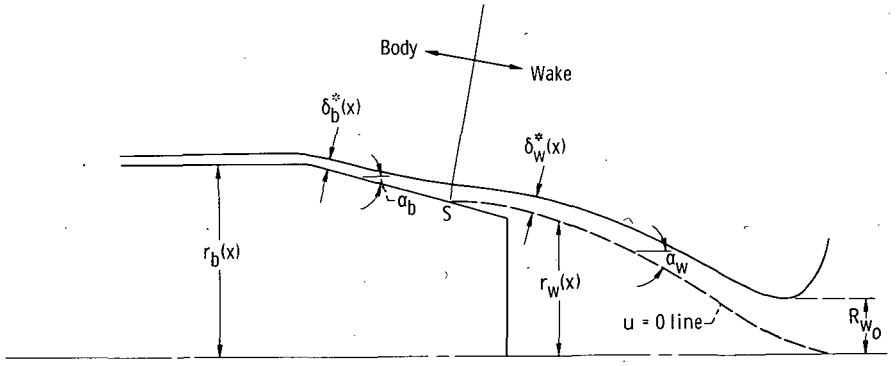

Figure 2. - "Wake-body" model (separation on body).

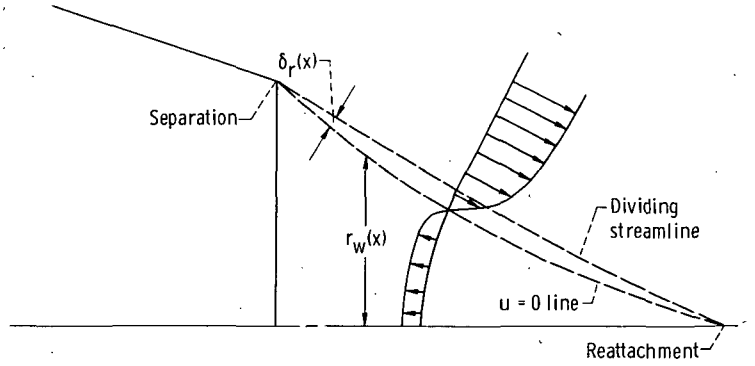

Figure 3. - Zero velocity line and dividing streamline in separated flow.

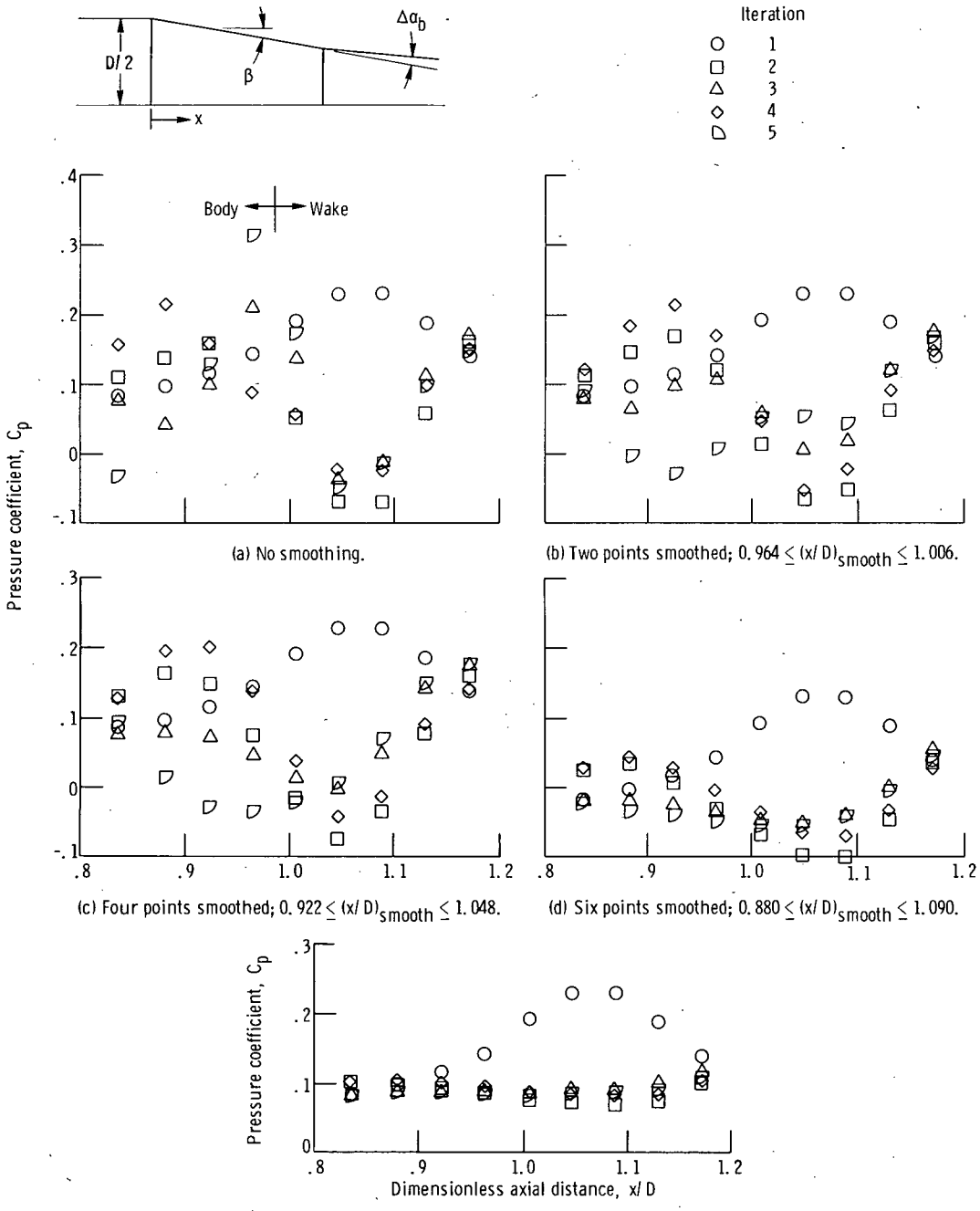

Figure 4. - Effect of smoothing displacement surface on pressure distribution in vicinity of base. Free stream Mach number $M_0 = 0.8$; boattail trailing edge angle $\beta = 10^0$; initial flow turning angle at base $\Delta\alpha_b = 5^0$.

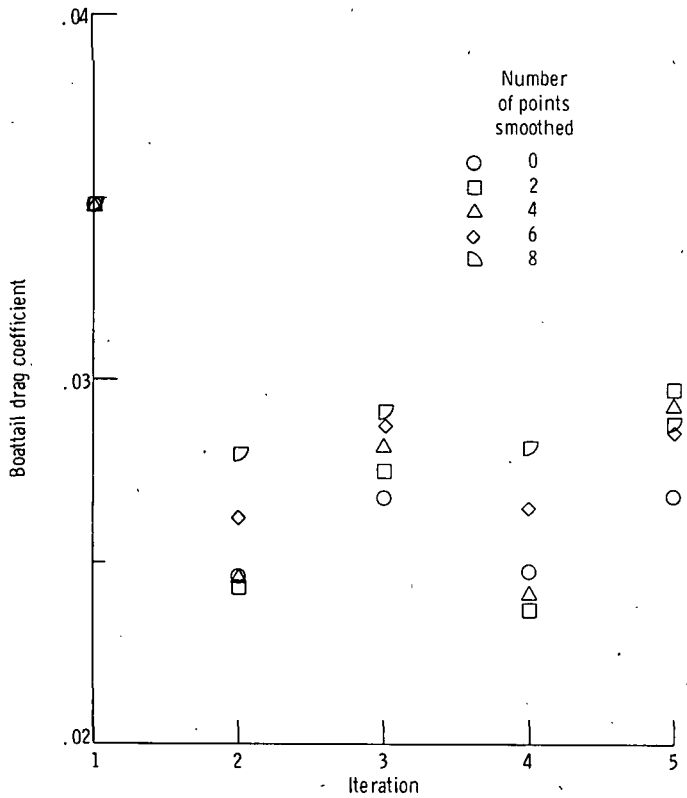

Figure 5. - Effect of smoothing displacement surface on convergence of computed boattail pressure drag coefficient. Free stream Mach number $M_0 = 0.8$; boattail trailing edge angle $\beta = 10^0$; initial flow turning angle at base $\Delta\alpha_b = 5^0$.

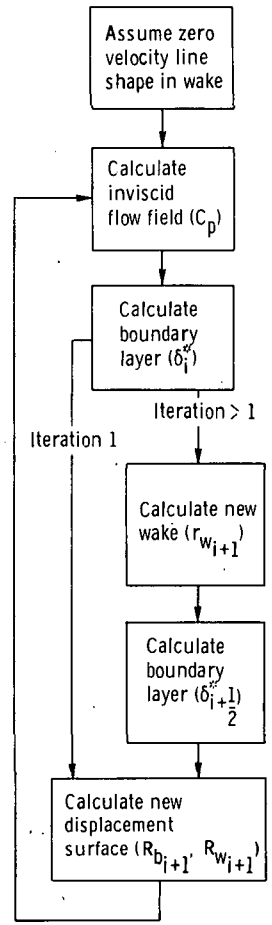

Figure 6. - Schematic of calculation procedure.

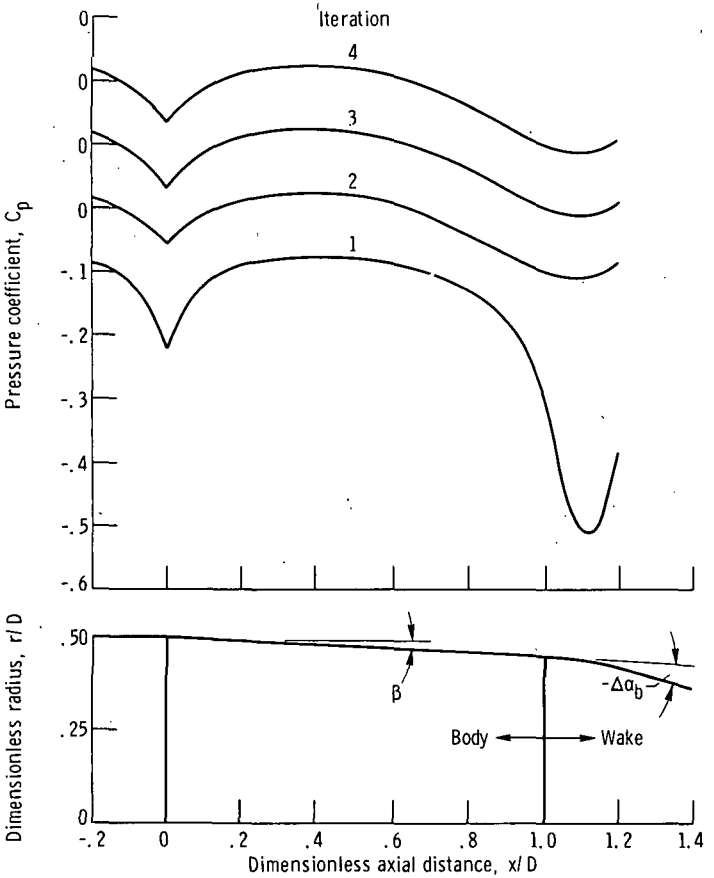

Figure 7. - Computed pressure distributions for first four iterations on 3^0 conical boattail. Free stream Mach number $M_0 = 0.8$; eight points smoothed $(0.767 \leq (x/D)_{smooth} \leq 1.227)$; initial flow turning angle at base $\Delta\alpha_b = -15^0$.

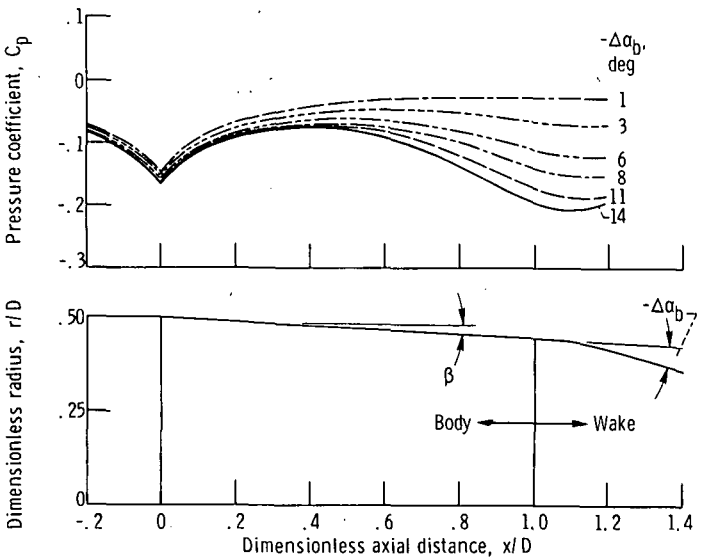

Figure 8. - Converged pressure distributions for several initial zero velocity line shapes. Free stream Mach number $M_0 = 0.8$; boattail trailing edge angle $\beta = 3^0$; eight points smoothed $(0.767 \leq (x/D)_{smooth} \leq 1.227)$; fourth iteration.

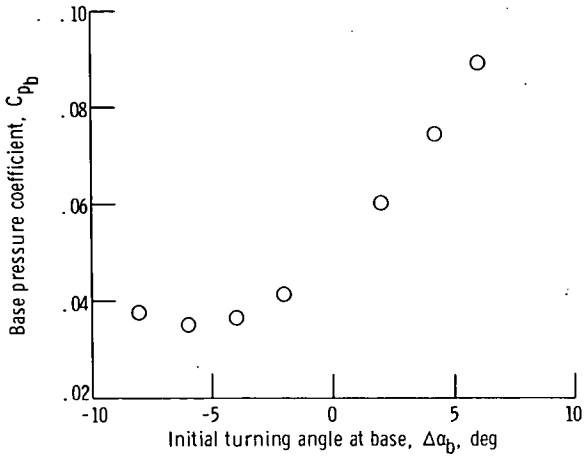

Figure 9. - Effect of initial turning angle at base on computed base pressure coefficient. Free stream Mach number $M_0 = 0.4$; boattail trailing edge angle $\beta = 10^0$; ten points smoothed ($0.783 \leq (x/D) \leq 1.172$); four iterations.

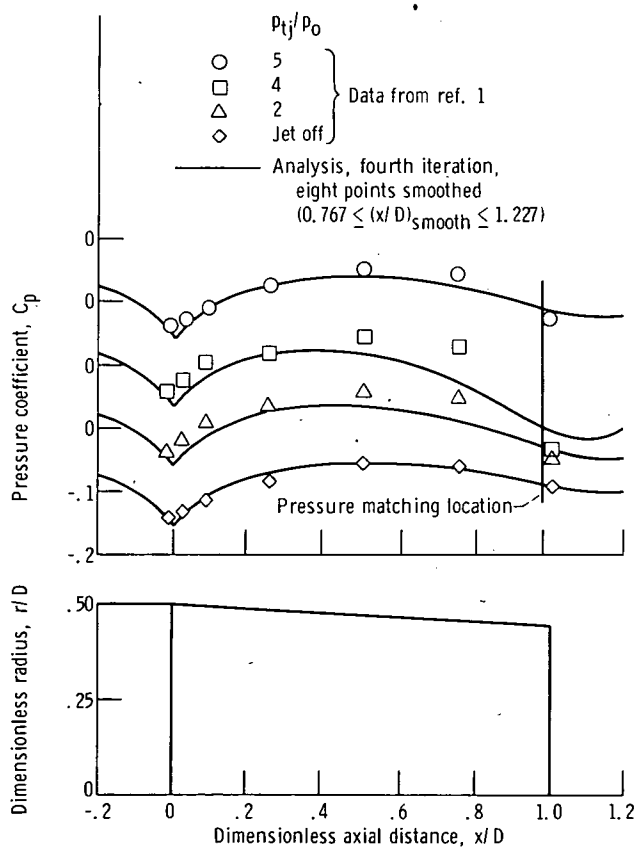

Figure 10. - Comparison of theoretical and experimental boattail pressure distributions for 3^0 conical boattail at free stream Mach number of 0.8.

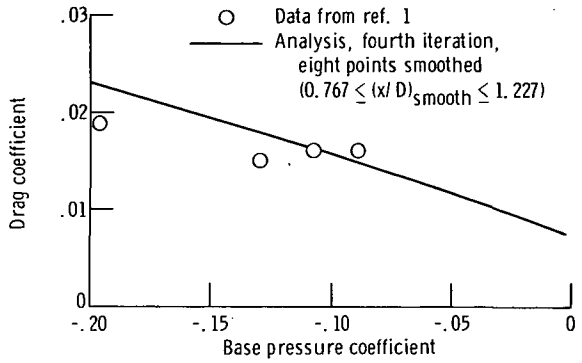

Figure 11. - Comparison of theoretical and experimental boattail pressure drag coefficients for 3^0 conical boattail at free stream Mach number of 0.8.

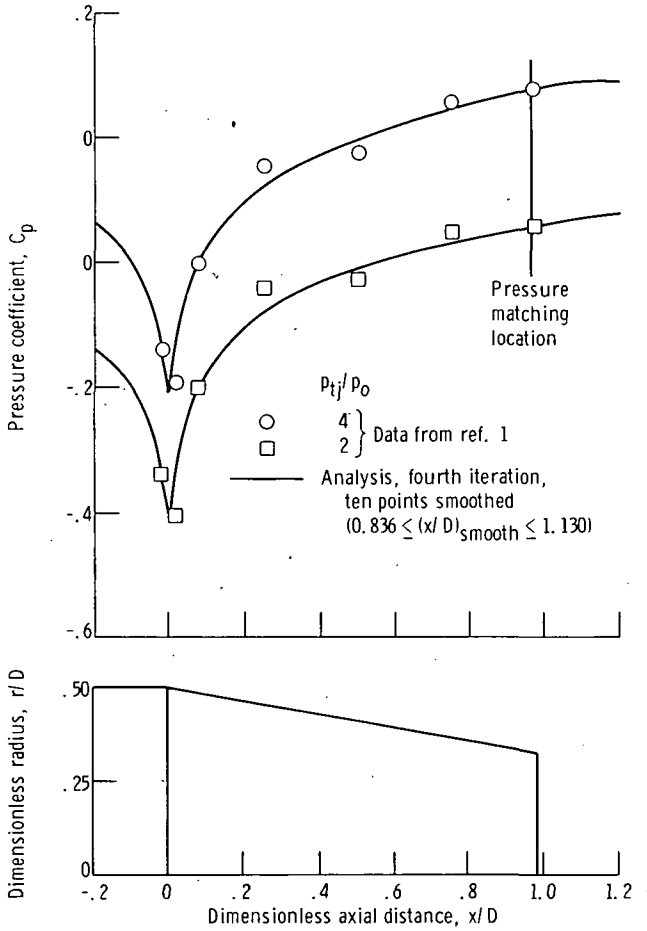

Figure 12. - Comparison of theoretical and experimental boattail pressure distributions for 10^0 conical boattail at free stream Mach number of 0.4.

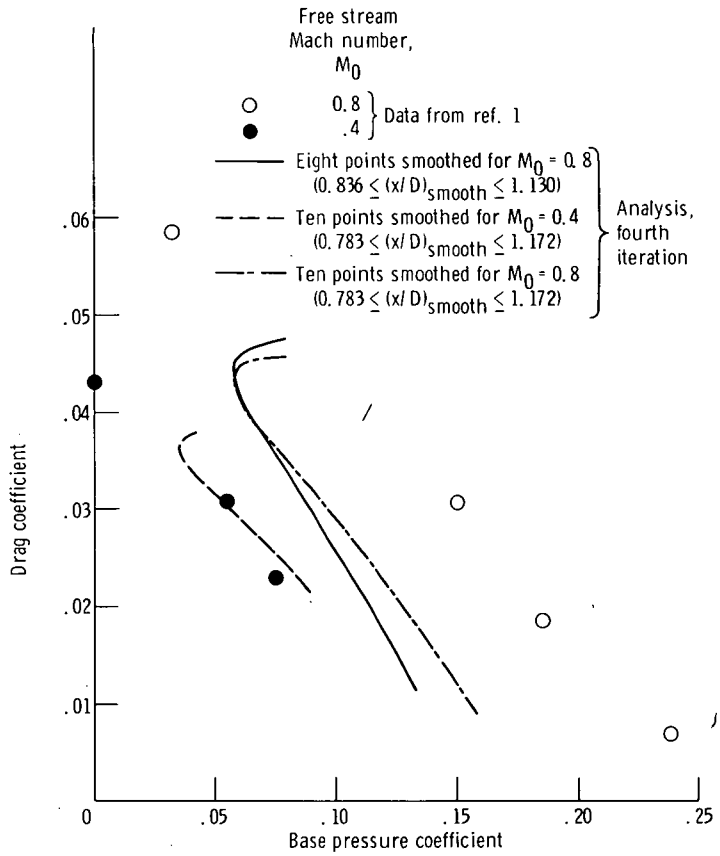

Figure 13. - Comparison of theoretical and experimental boattail pressure drag coefficients for 10^{o} conical boattail at free stream Mach numbers of 0.4 and 0.8.

NATIONAL AERONAUTICS AND SPACE ADMINISTRATION
WASHINGTON, D.C. 20546

OFFICIAL BUSINESS
PENALTY FOR PRIVATE USE $300

SPECIAL FOURTH-CLASS RATE
BOOK

POSTAGE AND FEES PAID
NATIONAL AERONAUTICS AND
SPACE ADMINISTRATION
451

U.S.MAIL

POSTMASTER: If Undeliverable (Section 158 Postal Manual) Do Not Return

"The aeronautical and space activities of the United States shall be conducted so as to contribute . . . to the expansion of human knowledge of phenomena in the atmosphere and space. The Administration shall provide for the widest practicable and appropriate dissemination of information concerning its activities and the results thereof."

—NATIONAL AERONAUTICS AND SPACE ACT OF 1958

NASA SCIENTIFIC AND TECHNICAL PUBLICATIONS

TECHNICAL REPORTS: Scientific and technical information considered important, complete, and a lasting contribution to existing knowledge.

TECHNICAL NOTES: Information less broad in scope but nevertheless of importance as a contribution to existing knowledge.

TECHNICAL MEMORANDUMS: Information receiving limited distribution because of preliminary data, security classification, or other reasons. Also includes conference proceedings with either limited or unlimited distribution.

CONTRACTOR REPORTS: Scientific and technical information generated under a NASA contract or grant and considered an important contribution to existing knowledge.

TECHNICAL TRANSLATIONS: Information published in a foreign language considered to merit NASA distribution in English.

SPECIAL PUBLICATIONS: Information derived from or of value to NASA activities. Publications include final reports of major projects, monographs, data compilations, handbooks, sourcebooks, and special bibliographies.

TECHNOLOGY UTILIZATION PUBLICATIONS: Information on technology used by NASA that may be of particular interest in commercial and other non-aerospace applications. Publications include Tech Briefs, Technology Utilization Reports and Technology Surveys.

Details on the availability of these publications may be obtained from:

SCIENTIFIC AND TECHNICAL INFORMATION OFFICE

NATIONAL AERONAUTICS AND SPACE ADMINISTRATION

Washington, D.C. 20546